

FROM ZO TO CO WITH DIFFRACTIONS: COMPLEX DATA EXAMPLES

A. Bauer, B. Schwarz and D. Gajewski

email: alex.bauer@uni-hamburg.de

keywords: common-offset, CRS, diffractions, stacking

ABSTRACT

The main goal of conventional seismic processing is to enhance and image reflections. Since reflected waves are not suitable for high-resolution structural imaging, diffractions are a key feature in seismic data. Diffracted waves behave physically different than reflected waves and carry important information about small-scale structures. In order to combine the stability of zero-offset processing with the improved illumination of common-offset processing, we introduced a straightforward decomposition principle for diffractions, which establishes a direct connection between zero-offset and common-offset wavefield attributes based on the decoupling of diffraction raypaths. The new method allows the direct prediction of common-offset diffraction attributes from the zero-offset section. Application to complex synthetic and marine field data reveals its ability to reliably image diffractions in the common-offset domain using only results from zero-offset processing as input. Particularly diffracted energy from sparsely illuminated areas is enhanced by the new method. The promising results in terms of both image and attributes reveal a high potential for improved pre-stack diffraction separation and diffraction-stereotomography.

INTRODUCTION

Conventional seismic processing techniques are designed to image and enhance reflection events. However, reflected waves are not suitable for high-resolution structural imaging of features below the Rayleigh limit of half a seismic wavelength (Dell and Gajewski, 2011). Information about these small-scale structures such as edges, faults, pinch-outs and small-size scattering objects is encoded in the diffraction response from the subsurface (Khaidukov et al., 2004; Fomel et al., 2007). Therefore, the imaging of diffracted waves, which behave physically different than reflected waves, is a crucial challenge in seismic processing.

Recently, different workflows with the goal to separate diffractions from reflections and to enhance diffraction imaging in the post-stack domain have been presented (Fomel et al., 2007; Berkovitch et al., 2009; Dell and Gajewski, 2011). However, an important goal of diffraction imaging is the separation of diffractions and their enhancement in the full pre-stack data volume, which requires common-offset diffraction processing. CO processing provides improved resolution, especially in sparsely illuminated regions such as subsalt areas, but it is computationally expensive, because the problem is of higher dimensionality than in the stable and commonly used zero-offset configuration.

In order to combine the stability of ZO CRS processing and the improved illumination of CO processing, Bauer et al. (2014) introduced a straightforward decomposition principle for diffractions. Based on the redundancy of zero-offset and common-offset information for diffractions, this new method allows the direct prediction of CO diffraction attributes from ZO CRS processing results. In this fashion, the full pre-stack data volume may be characterized without carrying out computationally expensive generic CO CRS processing (Zhang et al., 2001) or extrapolation by global application of ZO operators (partial CRS, Baykulov and Gajewski, 2009).

By fitting diffraction traveltimes and application to simple waveform data Bauer et al. (2014) showed that the new *common-offset prediction for diffractions* is able to accurately image diffractions for arbitrary offsets, whereas the ZO-based partial CRS (Baykulov and Gajewski, 2009) loses accuracy with offset. Comparison to the generic CO CRS reference (Zhang et al., 2001) proved the high quality of the CO prediction stack.

In this work, we apply the new method to complex synthetic and marine field data and compare the results to the ZO-based partial CRS and the generic CO CRS reference. We examine not only the predicted CO diffraction stacks and semblance sections, but also the quality of the predicted CO diffraction attributes.

COMPLEX SYNTHETIC EXAMPLE

We applied the CO prediction for diffractions to the synthetic Sigsbee 2A dataset, which is provided by the *Subsalt Multiples Attenuation and Reduction Technology Joint Venture (SMAART JV)*. The acoustic marine 2D model is based on the geological setting found in the Sigsbee escarpment in the Gulf of Mexico. Its key feature is a large homogeneous salt body, which is surrounded by stratified areas as found in typical sedimentary environments. The top of the salt body is very rugged and thus causes a lot of diffracted energy in the dataset, which contains a total of 2053 CMPs. In addition, the model contains two horizontal lines of equally spaced diffractors within the sedimentary structures left of and below the salt body. The Sigsbee 2A velocity model is displayed in Figure 1. For the calculation of the pre-stack data an absorbing free-surface condition and a weaker than normal water bottom reflection were used so that it does not contain free-surface multiples and less than normal internal multiples.

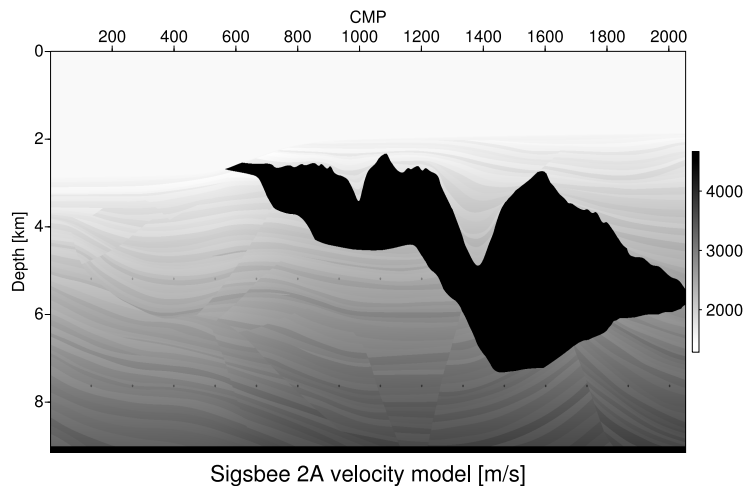


Figure 1: Velocity model of the synthetic Sigsbee 2A dataset.

For comparison, we also applied the ZO-based CO extrapolation method (partial CRS, Baykulov and Gajewski, 2009) and the generic CO CRS (Zhang et al., 2001) to the data. The goal of this investigation is to examine how the CO prediction performs on complex realistic data, which contains both reflected and diffracted energy and if the method is able to enhance diffractions and attenuate reflections. Tests showed that during the processing, a wise choice of apertures is crucial for obtaining the desired results (Bauer, 2014). Especially for the CO refinement carried out by CO prediction and CO extrapolation it is recommendable to use rather small stacking apertures.

Semblance and stack

Excerpts containing 900 CMPs (compare the velocity model in Figure 1) from the computed CO semblance sections obtained from the three methods are displayed in Figure 2. A comparison of figures 2(a) and 2(b) reveals that the CO prediction due to the application of a pure diffraction operator strongly attenuates reflected energy, particularly horizontally layered reflections as present directly below the sea floor.

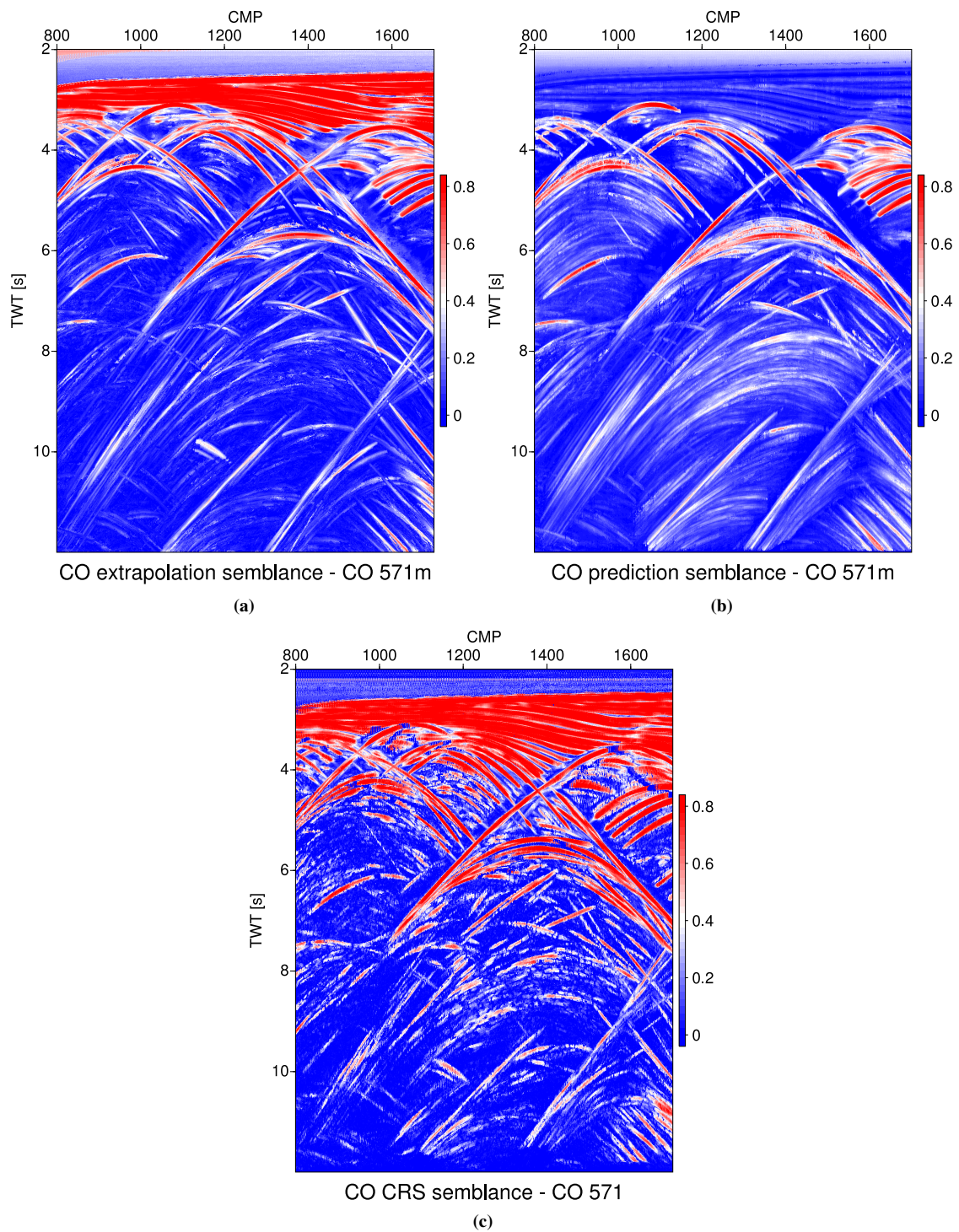


Figure 2: Excerpts of the Sigsbee 2A semblance sections for the offset 571 m obtained from (a) CO extrapolation (partial CRS), (b) CO prediction and (c) generic CO CRS.

However, diffracted energy is more present in the results obtained from CO prediction, especially in the responses which stem from the bottom of the salt body and from below of the salt. Whereas the diffraction hyperbolae caused by the top of the salt body look smoother and more coherent in the CO extrapolation results, diffracted energy from deeper parts of the model is more present in the predicted CO semblance section. Especially in the areas around CMP 1000 at 4.5 s and around CMP 1400 at 6 s, diffracted energy is more coherent in the predicted CO results.

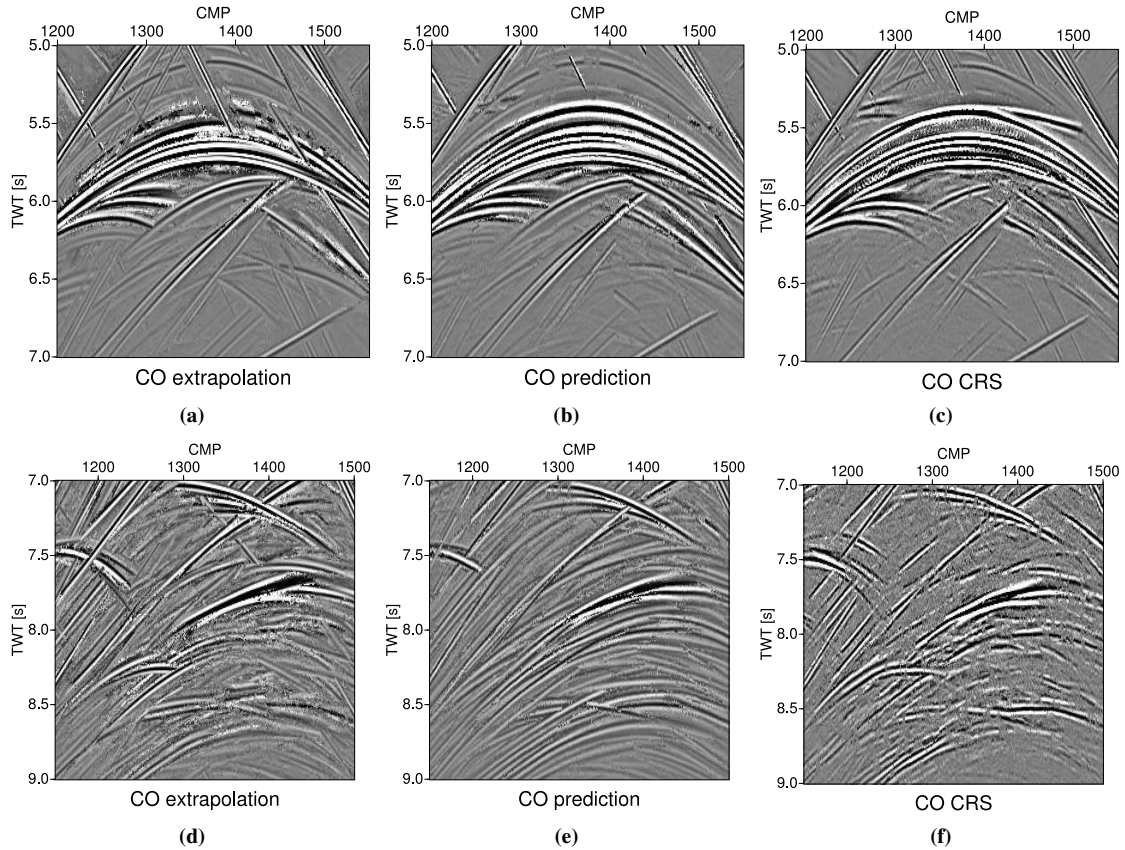


Figure 3: Excerpts of the Sigsbee 2A stacked sections for the offset 571 m displaying responses from the top of salt (above) and from the subsalt area (below). In both excerpts the quality of the CO prediction results (center) is better than the ZO-based CO extrapolation (partial CRS, left) and the generic CO CRS reference (right).

A comparison of the CO prediction result to the CO CRS reference displayed in Figure 2(c) reveals that the predicted CO section contains more coherent diffraction energy particularly in the parts of the model which are difficult to image: at the bottom and below of the salt body. Reflection energy, however, is more coherent in the CO CRS reference. These results show that the principle of the CO prediction for diffractions works and that the method is capable of fitting diffraction events in complex geological settings equally or even better than the generic CO reference. Note at this point that the prediction results were computed solely based on wavefield attributes obtained from the ZO section.

Figure 3 provides two excerpts of the stacks corresponding to the examined semblance sections for the three different methods. The excerpts are taken from sparsely illuminated areas from the top of salt and from the subsalt area, which contain much diffracted energy. The results clearly show that the CO prediction enhances diffracted energy, particularly in complex subsurface areas. In the first excerpt (Figure 3, above) the present diffraction hyperbolae are imaged more coherently by the CO prediction than by partial CRS. Also by generic CO CRS processing the diffractions are imaged slightly more blurry. On the diffracted energy from the deeper parts of the model present in the second excerpt (Figure 3, below) the

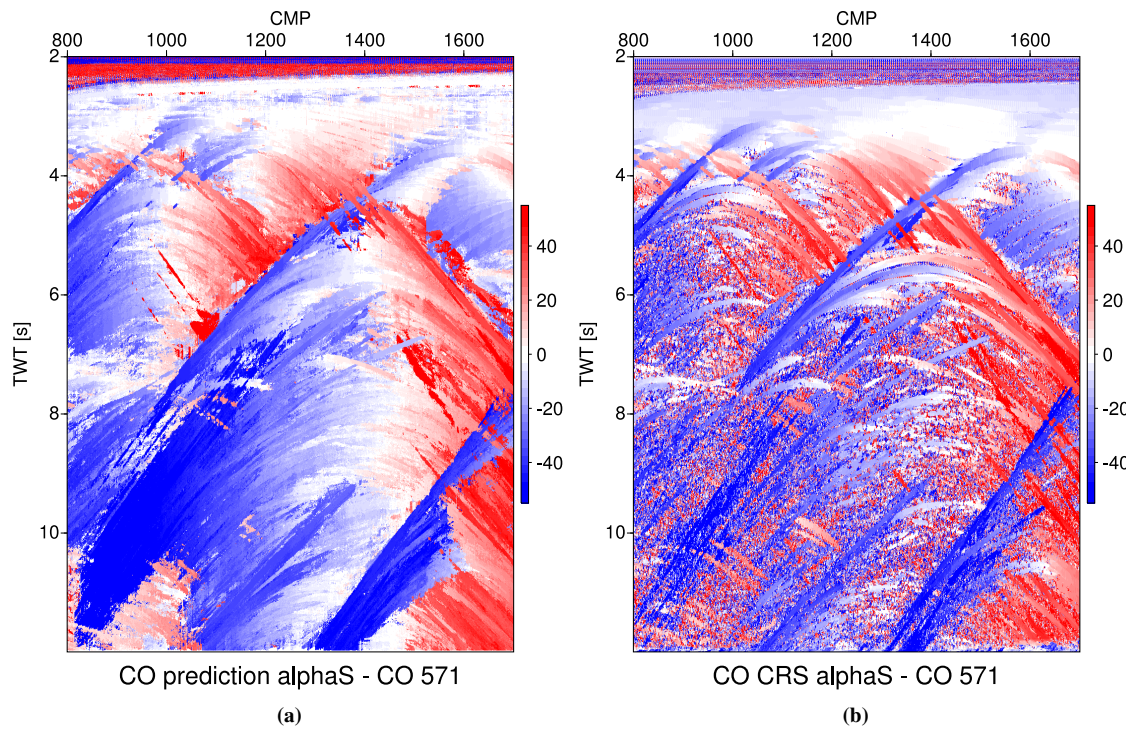


Figure 4: Sigsbee 2A: emergence angle at the source α_s [°] for the offset 571 m obtained from (a) CO prediction and (b) generic CO CRS.

CO prediction shows its strengths as these weaker responses are imaged more clearly and coherently than by the other two methods.

The results for the synthetic Sigsbee 2A dataset show that the CO prediction for diffractions is a powerful tool to image diffractions in the common-offset domain, given that the method only requires stacking results and wavefield attributes from zero-offset CRS processing. Despite of being ZO-based the quality of the CO diffraction imaging is equal to or even better than the CO CRS reference. In particularly in the sparsely illuminated subsalt area, the new method clearly enhances diffracted energy. Tests with different stacking apertures showed that whereas the CO prediction images diffractions even more clearly and more coherently using small midpoint apertures, for larger midpoint apertures it is able to attenuate reflections more effectively maintaining a relatively good diffraction fit (see Bauer, 2014).

Wavefield attributes

In order to examine the quality of the predicted CO wavefield attributes, we provide the predicted source attribute α_s (Figure 4(a)) and its respective CO CRS reference (Figure 4(b)). The wavefront curvatures are not shown, because a CO CRS reference cannot be provided due to the different parametrization used during the CO CRS processing (see Zhang et al., 2001). Since the observed effects would be the same as for their counterparts, the respective receiver attributes are not provided.

The quality of the predicted CO wavefield attributes mainly depends on the quality of the respective ZO attributes, because the CO diffraction operators are solely composed out of them. In order to favor the imaging of diffracted energy, it is recommended to choose relatively small offset and midpoint apertures for the ZO CRS processing (Bauer, 2014).

In compliance with the previous observations, the α_s -section obtained from CO prediction reveals that the method in general finds very well the angles which define the best fitting CO diffraction operators. Problems finding the CO attributes occur in conflicting dip situations, particularly where the contributions from various events interfere (compare e.g. CMP 1000 at 6 s and CMP 1200 at 10 s). A comparison of the predicted CO source angle section with the respective CO CRS reference (see Figure 4(b)) reveals the high

quality of the predicted CO diffraction attributes. Where the CO CRS processing found coherent events, the corresponding angle values coincide almost perfectly with the predicted ones. The overall quality of the predicted CO diffraction attributes is higher than the quality of the CO CRS angles as the predicted angle section appears more coherent, particularly in the responses from the subsalt area.

Computation times

A comparison of the methods' computation times for the results on the Sigsbee 2A dataset reveals striking differences to the application to simple waveform data, where the CO prediction was very fast (see Bauer et al., 2014). Since it neither requires optimization nor a search for events, the CO extrapolation method (partial CRS, Baykulov and Gajewski, 2009) is the fastest method. Together with the necessary prior ZO CRS processing partial CRS on Sigsbee 2A needed 70 % of the CO CRS computation time. On complex data, the new CO prediction for diffractions is the computationally most expensive method. Here, ZO CRS processing and subsequent CO prediction required 429 % of the generic CO CRS processing time. The CO prediction computation time depends on its input parameters and on the number of events present in the data, because for each event found on the source trace all possible event combinations with events from the receiver trace lying within the t_0 search range (Bauer et al., 2014) have to be tested in order to find the two best matching events. This process is computationally expensive on complex data. However, note at this point that the primary goal of the current implementation was the examination of the method's functionality and not its performance in terms of computation time. Undoubtedly, the code may be optimized in several ways, for instance by defining confinements for the attribute combinations. Also, the implementation could be subject to parallelization.

FIELD DATA EXAMPLE

As a next step, we applied the ZO-based common-offset prediction for diffractions to a marine 2D field data set. The dataset provided by TGS was recorded in 2009 in the Levantine Basin, which is located in the Eastern Mediterranean Sea to the south of Cyprus. For the results presented in this work, an excerpt of the dataset was used.

As before, the two ZO-based methods CO extrapolation (partial CRS, Baykulov and Gajewski, 2009) and CO prediction as well as the generic CO CRS stack (Zhang et al., 2001) were applied to the data. Again, the stacking apertures were chosen relatively small because this favors the imaging of diffractions (Bauer, 2014).

Semblance and stack

Figure 5 shows the CO semblance sections of the marine field data generated by CO extrapolation, CO prediction and generic CO CRS processing, respectively. A comparison of the CO prediction semblance with the CO extrapolation semblance reveals that the CO prediction images the diffracted energy more coherently (compare CMPs 2620 to 2900 at 2-3 s). A larger difference in the quality of the fit favoring the CO prediction is visible in the multiples of the diffractions from below the seafloor (compare CMPs 2620 to 2900 at 4 s). In general, diffracted energy present at larger traveltimes is imaged more coherently by the CO prediction. Reflections in general, but particularly the strong seafloor reflection is attenuated almost completely by the CO prediction for diffractions. At the seafloor multiple, however, the CO prediction images some coherent energy, although still less than the CO extrapolation.

Comparison of the CO prediction semblance to the CO CRS reference (see Figure 5(c)) again reveals the high quality of the CO prediction diffraction fit. The diffracted energy is imaged clearer and more coherently than by CO CRS processing, in particular at large traveltimes. Only the tails of some diffraction hyperbolae are not imaged by the CO prediction (compare CMP 2950 at 3.5 s). This is because they are not very coherently imaged in the ZO CRS result (not shown here, see Bauer, 2014), in which the CO prediction searches for the events.

Two excerpts of the respective stacked sections taken from the previously stressed areas, which contain diffracted energy from a salt body, are displayed in Figure 6. They basically confirm the observations made on the semblance sections. The CO prediction (center) images the apices of the diffracted hyperbolae in the previously indicated area more clearly and more coherently than the CO extrapolation (left sides). The

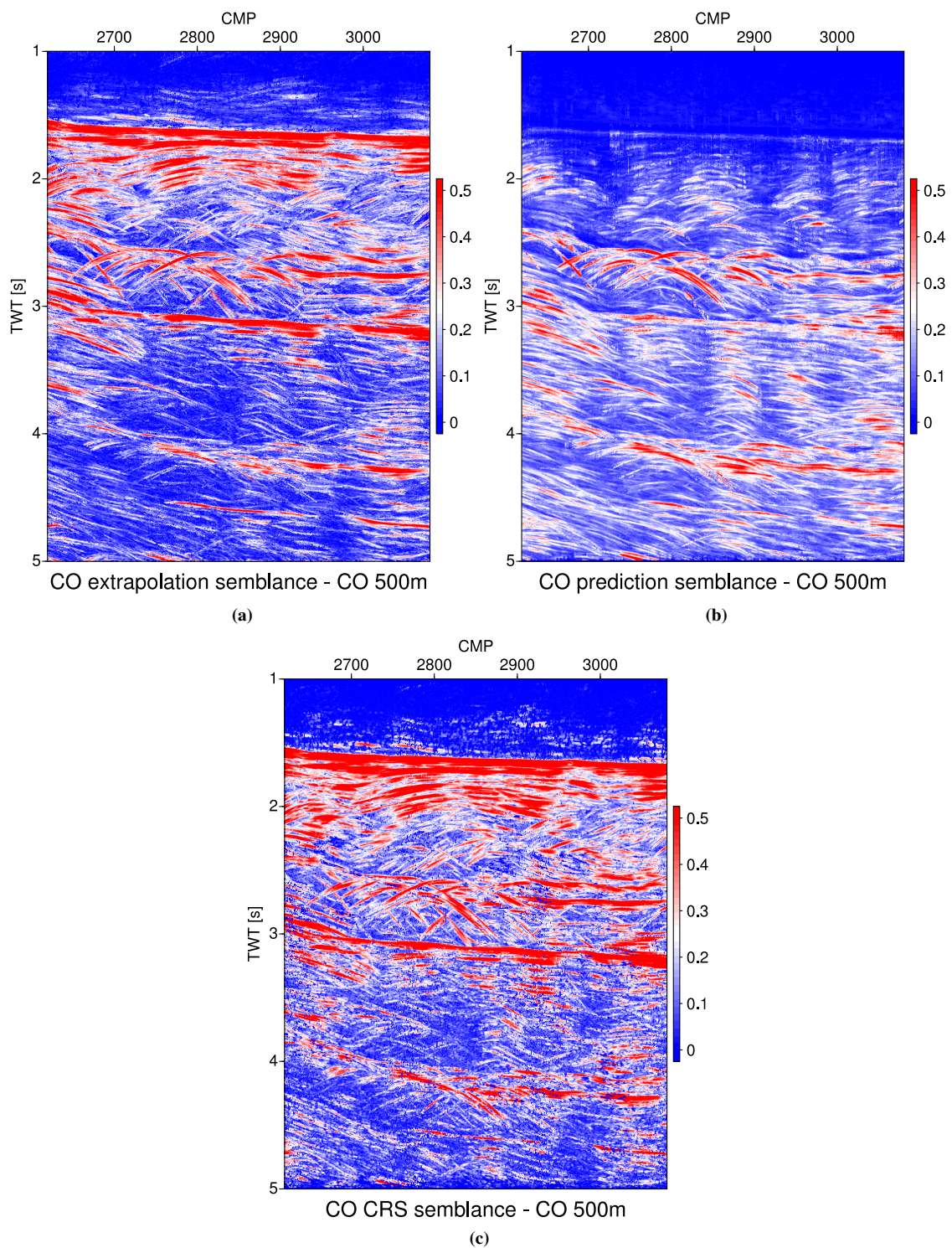


Figure 5: Semblance sections of the marine field data for the offset 500 m obtained from (a) CO extrapolation (partial CRS), (b) CO prediction and (c) generic CO CRS.

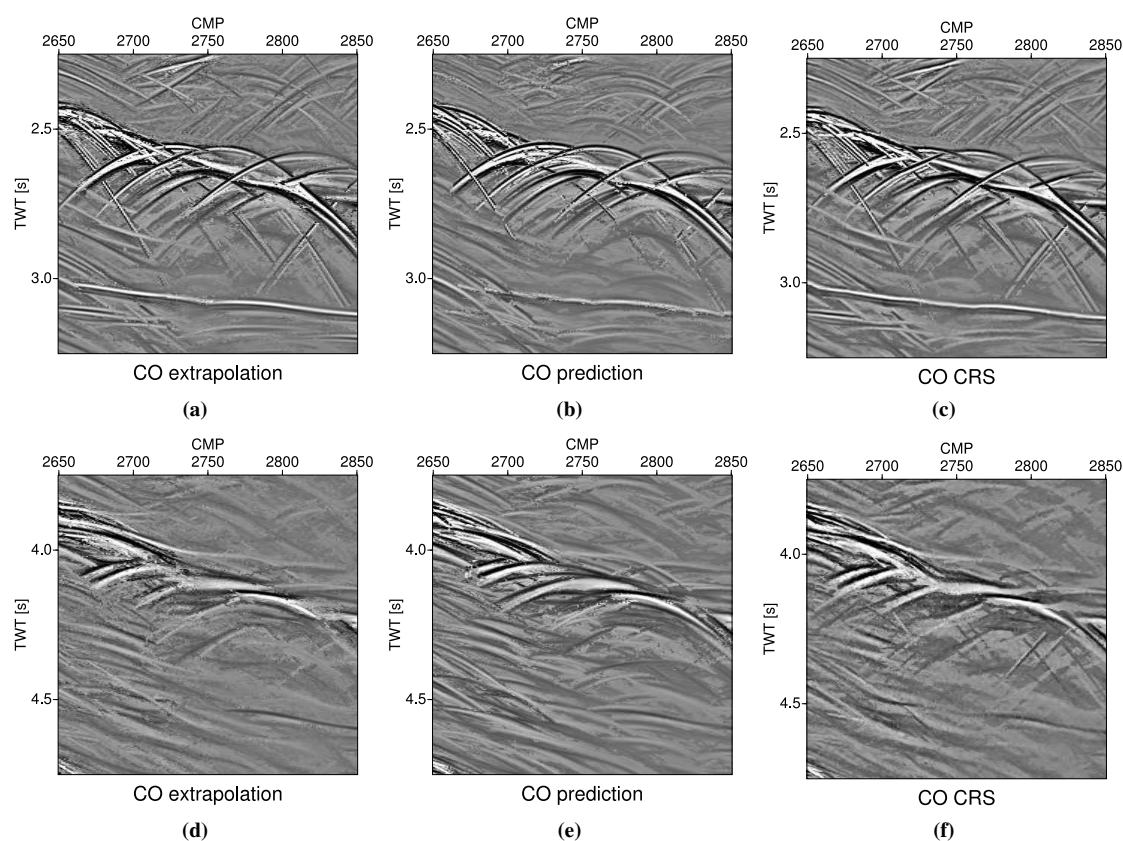


Figure 6: Excerpts of the field data stacks for the offset 500 m obtained from CO prediction (center), CO extrapolation (partial CRS, left) and CO CRS (right). The excerpts contain diffracted energy from a salt body (above) and the respective multiples (below).

weaker diffraction tails, however, are imaged better by the CO extrapolation. Diffracted energy visible at larger traveltimes is imaged more clearly by the CO prediction, whereas the new method images reflections very blurred. A closer look on the imaging of the reflected energy by the CO prediction (e.g. on the seafloor multiple in the second excerpt) reveals that the method tends to image nearly planar reflection events as various small hyperbolae. This kind of artifacts might be reduced by the use of pure diffraction stacking operators in the ZO CRS processing or by defining attribute confinements in order to avoid that the CO prediction tries to fit reflections. In the CO CRS reference (right sides), the apices of the diffraction hyperbolae are imaged a little less clearly than in the CO prediction stack, but on the other hand their tails are imaged better.

In conclusion, the stacking results on marine field data confirm the previously made observations and thus show the robustness of the new CO prediction for diffractions. Its drawbacks such as artifacts in reflection events and short tails of diffraction hyperbolae are basically caused by the input ZO results and thus might be fixed by improving the ZO processing in a way that favors diffraction imaging.

Wavefield attributes

Figure 7 shows the predicted CO source attribute α_s (left) and the respective CO CRS reference (right) for the field data.

The predicted α_s -section reveals the high quality of the attribute in those areas, where diffracted energy is imaged coherently. Diffraction tails are not always fully reproduced by the CO prediction, because the method is unable to find incoherently imaged events in the ZO results (see Bauer, 2014). As previously observed, the quality of the CO prediction attributes depends on the quality of the ZO processing results. If

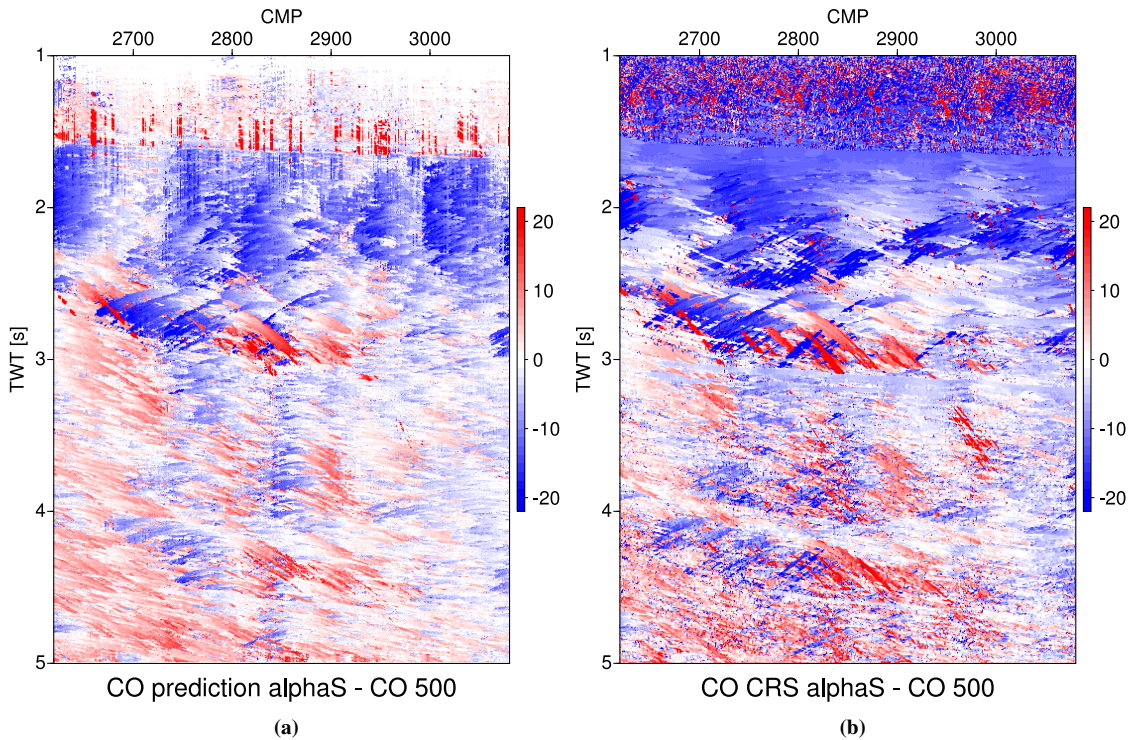


Figure 7: Field data: emergence angle at the source α_s [$^\circ$] for the offset 500 m obtained from (a) CO prediction and (b) generic CO CRS.

diffraction hyperbolae were imaged more coherently during the ZO processing, the CO prediction would be able to perfectly predict their CO counterparts. Accordingly, enhancing diffractions in the ZO processing will lead to fundamental improvement in the CO prediction results.

Comparison of the predicted angle to the CO CRS reference reveals good conformity of the attribute values for the diffracted energy in the data. Again, the predicted angle section appears more coherent at larger traveltimes, whereas the generic CO CRS angle is of higher quality along the tails of some diffraction hyperbolae.

The overall high quality of the predicted CO diffraction attributes favors their exploitation in future work, such as the development of a diffraction stereo-tomography.

Computation times

On this field dataset, relative to the CO CRS reference, the ZO CRS processing and the CO prediction were faster than on the Sigsbee 2A dataset, as they required 217 % of the CO CRS computation time. The generally fast ZO-based partial CRS method required, including the ZO CRS processing, 25 % of the CO CRS time. In addition to the choice of stacking parameters, the computation times of all of these three methods, in particular the CO prediction, strongly depend on the event content of the data. Accordingly, the computation time percentages stated in this work may only be seen as guiding values, which provide some insight into the methods' computational efficiency. As previously stressed, the implementation of the CO prediction may be subject to optimization in terms of speed in various ways, such as parallelization or further confinements of the computationally expensive event search.

CONCLUSIONS AND OUTLOOK

Application of the new *CO prediction for diffractions* to the complex synthetic Sigsbee 2A dataset revealed that also on complex data diffractions are imaged at the same or even higher quality than by the generic CO CRS stack. In particular, diffracted energy from the subsalt area is enhanced by the new ZO-based

method. Due to its use of pure diffraction operators the CO prediction is not only accurate for arbitrary offsets, but also intrinsically enhances diffractions and attenuates reflected energy. A comparison of the predicted CO diffraction wavefield attributes to the CO CRS reference revealed the high quality of the predicted attributes.

The subsequent application of the new method to marine field data confirmed the promising observations from the Sigsbee 2A results again revealing its potential to enhance diffractions, attenuate reflections and provide high quality CO diffraction attributes. Further, the results showed the strong dependence of the new method on the quality of the ZO CRS results, which serve as input.

In future work, the implementation of the CO prediction for diffractions may be subject to optimization in terms of computational effectivity, which was not the main focus of this work. This optimization may include the definition of confinements for the wavefield attributes during the search of matching events, which would also reduce the amount of artifacts in the results. A fundamental improvement of the new method is expected to be achieved by enhancing diffractions in the ZO processing, for instance by using different stacking operators, such as the non-hyperbolic i-CRS (Schwarz et al., 2014), or even pure diffraction operators. Thus, a reliable pre-stack diffraction separation could be achieved. Another update of the current implementation could be the integration of conflicting dip handling. Further, the high quality of the predicted CO diffraction wavefield attributes favors the future development of a diffraction-stereotomography.

ACKNOWLEDGMENTS

This work was kindly supported by the sponsors of the *Wave Inversion Technology (WIT) Consortium*, Karlsruhe, Germany. The synthetic Sigsbee 2A dataset was provided by the *Subsalt Multiples Attenuation and Reduction Technology Joint Venture (SMAART JV)*. The marine field data was kindly provided by TGS.

REFERENCES

- Bauer, A. (2014). From zero-offset to common-offset with diffractions. master's thesis, University of Hamburg.
- Bauer, A., Schwarz, B., and Gajewski, D. (2014). From ZO to CO with diffractions: Theory. *18th Annual WIT report*.
- Baykulov, M. and Gajewski, D. (2009). Prestack seismic data enhancement with partial common-reflection-surface (CRS) stack. *Geophysics*, 74:V49–V58.
- Berkovitch, A., Belfer, I., Hassin, Y., and Landa, E. (2009). Diffraction imaging by multifocusing. *Geophysics*, 74:WCA75–WCA81.
- Dell, S. and Gajewski, D. (2011). Common-reflection-surface-based workflow for diffraction imaging. *Geophysics*, 76:S187–S195.
- Fomel, S., Landa, E., and Taner, M. T. (2007). Diffraction imaging by multifocusing. *Geophysics*, 74:WCA75–WCA81.
- Khaidukov, V., Landa, E., and Moser, T. J. (2004). Diffraction imaging by focusing-defocusing: An outlook on seismic superresolution. *Geophysics*, 69:1478–1490.
- Schwarz, B., Vanelle, C., Gajewski, D., and Kashtan, B. (2014). Curvatures and inhomogeneities: an improved common-reflection-surface approach. *Geophysics*, 79:S231–S240.
- Zhang, Y., Bergler, S., and Hubral, P. (2001). Common-reflection-surface (CRS) stack for common offset. *Geophysical Prospecting*, 49:709–718.